ELSEVIER

Journal of Organometallic Chemistry 660 (2002) 85–90

Journal of Organometallic Chemistry

www.elsevier.com/locate/jorganchem

8-Sila-4-stanna-*s*-tetrahydroindacenes as synthons for Me_2Si-bridged zirconocenes: formation from biscyclopentadienyl silanes by reaction with aminostannanes

Mario Hüttenhofer, Frank Schaper, Hans-Herbert Brintzinger *

Fachbereich Chemie, Universität Konstanz, Universitätsstraße 10, Fach M 737, D-78457 Konstanz, Germany

Received 16 May 2002; received in revised form 19 June 2002; accepted 5 July 2002

Dedicated to Professor Gottfried Huttner on the occasion of his 65th birthday.

Abstract

Alkyl-substituted bis(cyclopentadienyl)dimethylsilanes react with $Me_2Sn(NEt_2)_2$ and with $(Me_2N)_4Sn$ to yield correspondingly substituted, *meso*-configurated *RS*-8-sila-4-stanna-*s*-tetrahydroindacene and axially symmetric *RR*,*SS*-4-spiro-bis(8-sila-4-stanna-*s*-tetrahydroindacene) compounds, respectively, which are stereoselectively converted by reaction with $ZrCl_4$ to the corresponding *meso*- and *rac*-configurated *ansa*-zirconocene complexes.

Keywords: Aminostannanes; Crystal structures; Axially symmetric

1. Introduction

Rac- and *meso*-configurated *ansa*-zirconocenes were structurally characterized for the first time by Huttner and coworkers in 1982 [1]. Since then, substantial efforts have been directed toward effective diastereoselective syntheses of silyl-bridged chiral *ansa*-zirconocenes [2] with the aim to obtain exclusively the *rac*-configurated complexes, which can be used as stereoselective polymerization catalysts [3,4], without concomitant formation and subsequent separation of the *meso*-configurated isomer. Remarkable progress in this regard has been achieved by Jordan and coworkers by use of zirconium amido precursors [5–8], by Damrau et al. with zirconium biphenolates [9], and by the groups of Nifant'ev and Resconi [10–12] and Lisowsky [13] through the use of distannylated bis(indenyl) derivatives as starting materials. We have observed that *meso*-configurated sila-stanna-tetrahydroindacene derivatives [14] react smoothly with $ZrCl_4$ to give, by stereoselective transfer of both cyclopentadienyl rings from Sn to Zr, high yields of the *meso*-configurated *ansa*-zirconocene diastereomers [15].

For the synthesis of racemic *ansa*-zirconocenes, racemic 8-sila-4-stanna-tetrahydroindacenes would be required. Reaction of substituted dimethylsilyl-bis(cyclopentadienyl) dilithium derivatives with Me_2SnCl_2 always gave *rac*–*meso* mixtures, however, from which the racemic isomers could not be isolated [15]. To find alternative routes to these compounds, we have investigated the use of aminostannanes as metallation reagents.

Aminostannanes, first prepared by Thomas [16] and by Lappert und Jones [17], were used by Lyle und Stobart [18] to connect cyclopentadiene ligands to a tin center. We have followed up on these reports to utilize reactions of aminostannanes with dimethylsilyl-bridged bis(cyclopentadienyl) compounds for the preparation for 8-sila-4-stanna-tetrahydroindacenes.

2. Results and discussion

Reactions of the dimethylsilyl-bridged compounds **1A**–**D** with bis(diethylamino) dimethyltin in diethyl

* Corresponding author. Tel.: +49-7531-882-629; fax: +49-7531-883-137

E-mail address: hans.brintzinger@uni-konstanz.de (H.-H. Brintzinger).

0022-328X/02/$ - see front matter
PII: S0022-328X(02)01775-8

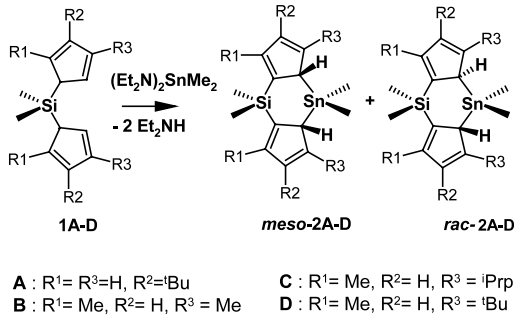

Scheme 1.

ether gave, in the course of 16–20 h, the expected tetrahydro-8-sila-4-stanna-indacenes **2A**–**D** (Scheme 1). ^{1}H-NMR spectra of the product mixtures obtained from these reactions indicate that the *meso* isomer of **2A** is even more strongly favored than in the reaction of the dimethylsilyl bis(cyclopentadienyl) dilithium derivative with Me_2SnCl_2, while for **2B** and **C** *meso*:*rac* ratios close to 1:1 arise from both reactions (Table 1). The methyl-*tert*-butyl-substituted compound **2D**, finally, is formed, albeit in low yield, only as the racemic isomer. A distannylated compound, which was the sole product of the reaction of $Me_2Si(Me\text{–}^tBu\text{–}C_5H_2Li)_2$ and Me_2SnCl_2, is now formed as a minor side product only.

Compound *rac*-**2D** was characterized by a crystallographic structure determination (Fig. 1, Table 2). Both crystallographically independent molecules contained in the elementary cell of *rac*-**2D** are disordered with repect to rotation of one of their *tert*-butyl groups. Some steric strain due to the bulky *tert*-butyl groups is indicated by a widening of the central six-membered ring, with the angle Sn1–C1–C2 being reduced to an unusually small value of 96°, and by a twisting of the dimethyltin plane C21–Sn1–C22 away from its normal orientation perpendicular to the plane C1–Sn1–C6 by 5°.

Reaction of two equivalents of the silyl-bridged compound **1A** with the tin tetraamide $Sn(NMe_2)_4$ gives rise to the tin spiro compound $Me_2Si(3\text{-}^tBu\text{–}C_5H_3)_2Sn(3\text{-}^tBu\text{–}C_5H_3)_2SiMe_2$ [19]. A crystallographic structure determination of compound **3A** (Fig. 2, Table 3) reveals a geometry with approximate S_4 symmetry, which implies opposite configurations of the two C_2-symmetric sila-stanna-tetrahydroindacene units connected at the spiro-Sn center. The structure deviates slightly from S_4 symmetry in that the axes Si(1)–Sn and Sn–Si(2) of the two sila-stanna-tetrahydroindacene units form an angle of 162° at the Sn center. The approximate S_4 symmetry of isomer *RR*,*SS*-**3A** obviously accommodates the two *tert*-butyl-substituted sila-stanna-tetrahydroindacene units with less mutual repulsion than any other isomer.

To clarify which factors contribute to the strongly preferred formation of isomer *RR*,*SS*-**3A** from **1A** and $Sn(NMe_2)_4$, we have tried to obtain spectral data on the reaction intermediate $Me_2Si(^tBu\text{–}C_5H_3)_2Sn(NMe_2)_2$ (**4A**), which must precede formation of the spiro product **3A**. Even in 1:1 mixtures of $Sn(NMe_2)_4$ and **1A**, however, NMR spectra measured at short reaction times gave no indication for the presence of such an intermediate. Only signals due to the starting materials and to the final product **3A** were detected. This shows that formation of intermediate **4A** from $Sn(NMe_2)_4$ and **1A** is slower than its reaction with a second molecule of **1A** and, hence, rate-determining for the generation of the spiro product **3A** (Scheme 2).

Table 1
rac:*meso*-Ratios and isolated yields (in parentheses) of compounds **2A**–**D** as prepared by alternative reaction routes

	$Me_2Si(R_1R_2R_3C_5\text{-}HLi)_2 + Me_2SnCl_2$	$Me_2Si(R_1R_2R_3C_5\text{-}H_2)_2 + Me_2Sn(NEt_2)_2$
2A	1:2 (25%)	1:6 (82%)
2B	1:1 (40%)	1:1 (45%)
2C	1:1 (40%)	1:1 (41%)
2D		1:0 (25%) [a]

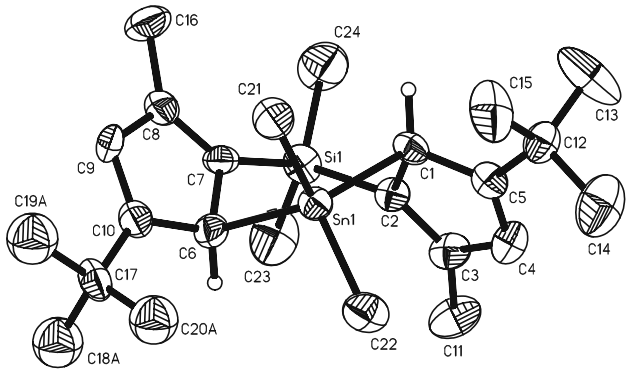

Fig. 1. Crystal structure of compound **2D** (thermal ellipsoids drawn at 50% probability, H atoms, disordered atoms and the second independent molecule in the asymmetric unit omitted for clarity).

Table 2
Selected bond distances (pm) and angles (°) for compound **2D** [a]

Bond distances	
Sn(1)–C(1)/Sn(2)–C(25)	221.5(7)/221.0(7)
Sn(1)–C(6)/Sn(2)–C(30)	220.5(8)/222.8(8)
Si(1)–C(2)/Si(2)–C(26)	185.1(8)/186.1(8)
Si(1)–C(7)/Si(2)–C(31)	185.9(8)/186.1(8)
C(1)–C(2)/C(25)–C(26)	151.8(10)/151.1(10)
C(2)–C(3)/C(26)–C(27)	135.2(11)/137.6(11)
Bond angles	
C(21)–Sn(1)–C(22)/C(45)–Sn(2)–C(46)	116.2(4)/117.6(4)
C(6)–Sn(1)–C(1)/C(25)–Sn(2)–C(30)	109.3(3)/110.4(3)
C(21)–Sn(1)–C(1)/C(46)–Sn(2)–C(25)	109.5(3)/108.5(3)
C(22)–Sn(1)–C(1)/C(45)–Sn(2)–C(25)	105.9(3)/105.1(3)
C(22)–Sn(1)–C(6)/C(45)–Sn(2)–C(30)	110.4(3)/110.0(3)
C(21)–Sn(1)–C(6)C(46)–Sn(2)–C(30)	105.5(3)/105.3(3)
Sn(1)–C(1)–C(2)/Sn(2)–C(25)–C(26)	96.1(5)/95.7(5)

[a] Two independent molecules are found in the asymmetric unit.

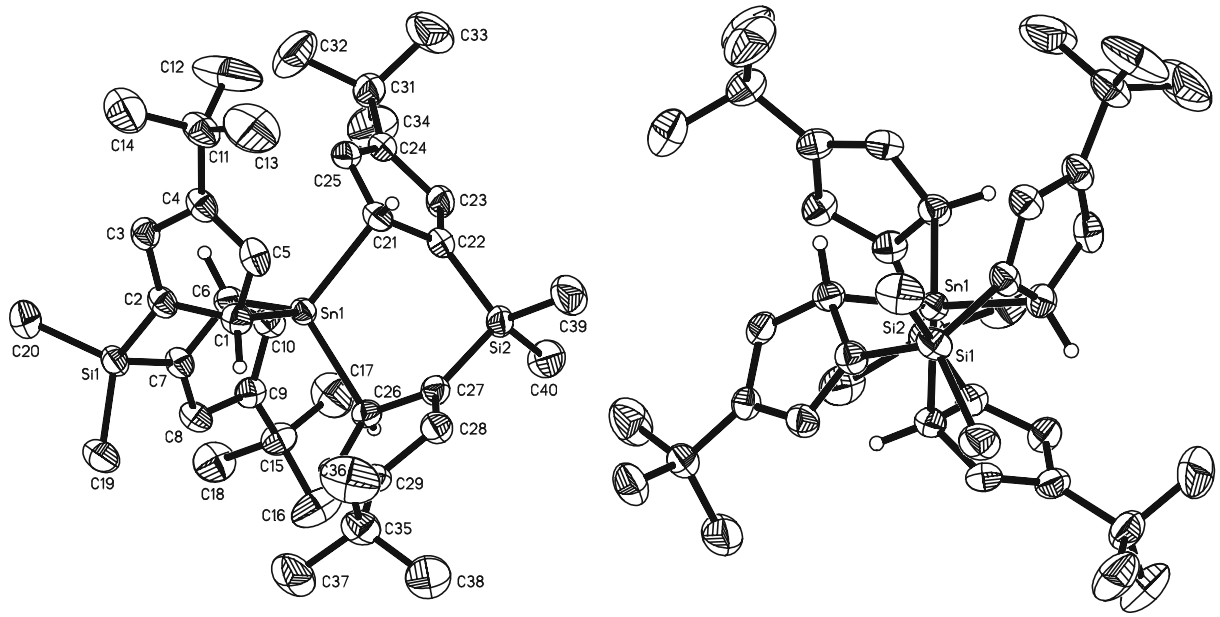

Fig. 2. Crystal structure of compound **3A** (thermal ellipsoids drawn at 50% probability, H atoms omitted for clarity, except for those at Sn-bound stereogenic C atoms).

Table 3
Selected bond distances (pm) and angles (°) for compound **3A**

Bond distances	
Sn(1)–C(1)	220.4(2)
Sn(1)–C(6)	219.6(2)
Sn(1)–C(21)	219.7(2)
Sn(1)–C(26)	220.3(2)
Si(1)–C(2)	186.0(3)
Si(1)–C(7)	185.8(3)
Si(2)–C(22)	185.5(3)
Si(2)–C(27)	185.6(3)
C(1)–C(2)	148.8(4)
C(2)–C(3)	136.0(4)
C(6)–C(7)	148.6(3)
C(7)–C(8)	136.6(4)
Bond angles	
C(1)–Sn(1)–C(6)	108.8(1)
C(1)–Sn(1)–C(21)	110.6(1)
C(1)–Sn(1)–C(26)	108.8(1)
C(6)–Sn(1)–C(21)	110.0(1)
C(6)–Sn(1)–C(26)	108.4(1)
C(21)–Sn(1)–C(26)	110.1(1)
C(2)–C(1)–Sn(1)	100.3(2)
C(7)–C(6)–Sn(1)	97.5(2)
C(22)–C(21)–Sn(1)	101.7(2)
C(27)–C(26)–Sn(1)	98.6(2)

The exclusive formation of the axially symmetric isomer *RR*,*SS*-**3A** thus requires that intermediate **4A** arises solely in form of its axially symmetric *rac* isomer. The stereoselective formation of *rac*-$Me_2Si(^tBu–C_5H_3)_2Sn(NMe_2)_2$ is reminiscent of the reaction between $Me_2Si(indH)_2$ and $Zr(NMe_2)_4$, which has been found by Jordan and coworkers to give preponderantly the *rac*-isomers of chiral *ansa*-zirconocenes such as $Me_2Si(ind)_2Zr(NMe_2)_2$ [5–7]. Since these authors had observed that complete formation of the racemic isomer required prolonged equilibration of the reaction participants with dimethylamine, we have also investigated effects of changing reaction conditions, such as closing the reaction vessel or sweeping the dimethylamine product out of the reaction mixture by a stream of N_2. In all cases, however, only immediate and complete formation of *RR*,*SS*-**3A** was observed. Under our reaction conditions, the *rac*-isomer of intermediate **4A** thus appears to be favored both in kinetic and in thermodynamic terms.

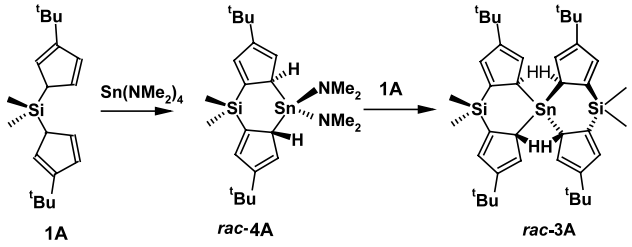

Scheme 2.

This preference for the formation of *rac*-**4A** from **1A** and $Sn(NMe_2)_4$ is unexpected in view of the exclusive formation of the *meso*-isomer of **2A** from **1A** and $Me_2Sn(NEt_2)_2$. To probe the origin of this reversal of stereochemical preference, we have calculated relative energies for the *meso* and *rac* isomers of **2A** and **4A** by semiempirical methods (PM3, Hyperchem 5.1). In accord with the experimental results, the *meso* isomer of complex **2A** is found to be more stable than its *rac* isomer by 0.5 kJ mol^{-1}. Replacement of the Me_2Sn fragment by $(Me_2N)_2Sn$, on the other hand, renders the

rac isomer of **4A** more stable than its *meso* isomer by 9 kJ mol^{-1}. This preference of intermediate **4A** for an axially symmetric geometry appears to be due to increased repulsive interactions of the spatially demanding NR_2 substituents with the substituted C_5 rings in a C_S symmetric *meso* isomer.

Reaction of the axially symmetric spiro compound **3A** with two equivalents of $ZrCl_4$ has been found to lead exclusively to the racemic isomer of $Me_2Si(3\text{-}^tBu\text{–}C_5H_3)_2ZrCl_2$ (Scheme 3) [19]. Our present studies show that axially symmetric tetrahydro-8-sila-4-stanna-indacene and spiro-bis(tetrahydro-8-sila-4-stanna-indacene) compounds are cleanly accessible, for use as synthons for the stereoselective preparation of *ansa*-zirconocenes, by reaction of a silyl-bridged ligand molecule with a tin amide such as $Me_2Sn(NEt_2)_2$ or $(Me_2N)_4Sn$, respectively.

3. Experimental

3.1. General procedures

All manipulations were performed on an argon/vacuum manifold or in a glovebox under a purified nitrogen atmosphere. Solvents were dried and distilled from sodium benzophenone. The Me_2Si-bridged ligand compounds $Me_2Si(3\text{-}^tBu\text{–}C_5H_4)_2$ (**1A**), $Me_2Si(2,4\text{-}Me_2C_5H_3)_2$ (**1B**) and $Me_2Si(2\text{-}Me\text{-}4\text{-}^tBu\text{–}C_5H_3)_2$ (**1C**) [20,21] and the tin amides $Me_2Sn(NEt)_2$ and $Sn(NMe_2)_4$ [22] were prepared as previously described. NMR spectra were recorded on Bruker AC 250 and DRX 600 spectrometers, with ^{1}H-NMR chemical shifts determined by comparison with residual ^{1}H solvent peaks. Peaks were assigned by HMQC and ROESY spectra. For ^{119}Sn-NMR, $SnMe_4$ was used as external standard. Elemental analyses were obtained on a Leybold–Heraeus Analysator.

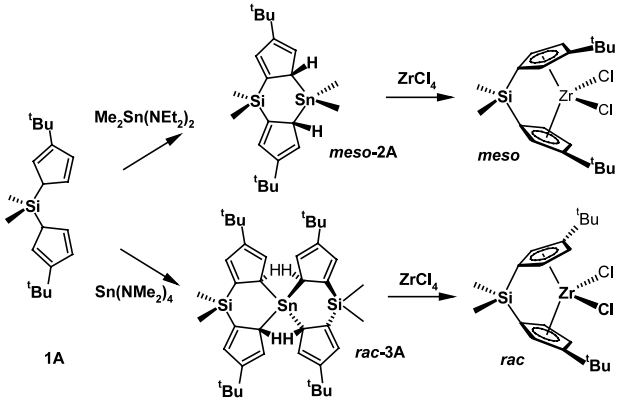

Scheme 3.

3.2. meso-2,6-Di-tert-butyl-4,4,8,8-tetramethyl-8-sila-4-stanna-tetrahydro-s-indacene (2A)

A solution of 2.48 g (8.5 mmol) bis(diethylamino)dimethylstannane in 25 ml of diethyl ether was added dropwise to a solution of 2.6 g (8.7 mmol) of dimethylbis(3-*tert*-butyl-cyclopentadienyl)silane in 100 ml of diethyl ether over a period of ca. 20 min, during which the initially light yellow solution turned to a golden yellow. ^{1}H-NMR spectra of the reaction mixture revealed formation of the *meso* and *rac* isomers of **3A** in a ratio of 6:1. After stirring overnight, the solvent and all volatiles were completely removed in vacuo and replaced by 20 ml of diethyl ether. Storage for 7 days at 0 °C and collection of the crystalline precipitate gave 2.9 g (6.9 mmol, 82% theoretical yield) of *meso*-**2A**. ^{1}H-NMR ($CDCl_3$, 600 MHz): δ 6.72 (s, 2H, $J(^1H\text{–}^{119}Sn)$ 18 Hz), 6.32 (s, 2H), 4.33 (s, 2H, $J(^1H\text{–}^{119}Sn)$ 100 Hz) 1.13 (s, 18H), 0.60 (s, 3H, $J(^1H\text{–}^{119}Sn)$ 51 Hz), 0.53 (s, 3H), 0.35 (s, 3H), −1.15 (s, 3H, $J(^1H\text{–}^{119}Sn)$ 55 Hz), in accord with [15].

3.3. meso-1,3,4,4,5,7,8,8-Octamethyl-8-sila-4-stanna-tetrahydro-s-indacene (2B)

A solution of 4.0 g (13.7 mmol) of bis(diethylamino)dimethylstannane in 40 ml of diethyl ether was reacted, as described above for **2A**, with a solution of 3.3 g (13.6 mmol) of dimethylbis(2,4-dimethylcyclopentadienyl)silane in 50 ml of diethyl ether. The golden yellow reaction mixture contained, as determined by ^{1}H-NMR, the *meso* and *rac* isomers of **2B** in a ratio of 1:1. Work-up as described above gave 2.4 g (6.1 mmol, 45% theoretical yield) of crystalline *meso*-**2B**. ^{1}H-NMR ($CDCl_3$, 600 MHz): δ 5.94 (s, 2H), 4.04 (s, 2H, $J(^1H\text{–}^{119}Sn)$ 80 Hz), 2.13 (s, 6H, $J(^1H\text{–}^{119}Sn)$ 18 Hz), 2.08 (s, 6H), 0.68 (s, 3H), 0.6 (s, 3H, $J(^1H\text{–}^{119}Sn)$ 42 Hz), 0.33 (s, 3H), −1.05 (s, 3H, $J(^1H\text{–}^{119}Sn)$ 43 Hz), in accord with [15].

3.4. meso-3,5-Di-isopropyl-1,4,4,7,8,8-hexamethyl-8-sila-4-stanna-tetrahydro-s-indacene (2C)

Reaction of 4.0 g (13.7 mmol) of bis(diethylamino)dimethylstannane in 40 ml of diethyl ether with 4.1 g (13.6 mmol) of dimethylbis(2-methyl-4-isopropylcyclopentadienyl)silane in 50 ml of diethylether, as described above, gave a solution containing *meso*- and *rac*-**2C** in a ratio of ca. 1:1. Work-up as described above gave 2.50 g (5.59 mmol, 41% theoretical yield) of crystalline *meso*-**2C**. ^{1}H-NMR ($CDCl_3$, 600 MHz): δ 6.00 (s, 2H, $J(^1H\text{–}^{119}Sn)$ 18 Hz), 4.23 (s, 2H, $J(^1H\text{–}^{119}Sn)$ 92 Hz), 2.58 (s, 2H), 2.14 (s, 6H, $J(^1H\text{–}^{119}Sn)$ 19 Hz), 1.15 (d, 6H, $J(^1H\text{–}^1H)$ 7 Hz), 1.11 (d, 6H, $J(^1H\text{–}^1H)$ 7 Hz), 0.65 (s, 3H), 0.54 (s, 3H, $J(^1H\text{–}^{119}Sn)$ 48 Hz), 0.35 (s, 3H), −1.02(s, 3H, $J(^1H\text{–}^{119}Sn)$ 53 Hz), in accord with [15].

3.5. *rac*-3,5-Di-*tert*-butyl-1,4,4,7,8,8-hexamethyl-8-sila-4-stanna-tetrahydro-*s*-indacene (**2D**)

A solution of 0.88 g (3.0 mmol) of bis(diethylamino)dimethylstannane in 30 ml of diethyl ether was reacted, as described above, with a solution of 1.0 g (3.0 mmol) of dimethyl-bis(2-methyl-4-*tert*-butylcyclopentadienyl)silane in 60 ml of diethyl ether. After stirring for 4 days at room temperature, the reagents were no longer detectable by ^{1}H-NMR. Apart from the indacene reaction product, the solution contained only minor amounts of distannylated biscyclopentadienylsilane. Complete removal of solvent and all volatiles in vacuo, dissolution of the residue in 5–10 ml of diethyl ether and storage for 21 days at −30 °C gave 350 mg (0.75 mmol, 25% theoretical yield) of crystalline *rac*-**2D**. ^{1}H-NMR ($CDCl_3$, 250 MHz): δ 6.24 (s, 2H, H–C_5, $J(^1H-^{119}Sn)$ 14 Hz), 4.66 (s, 2H, H–C_5, $J(^1H-^{119}Sn)$ 64 Hz), 2.20 (s, 6H, Me_{ring}, $J(^1H-^{119}Sn)$ 10 Hz), 1.14 (s, 18H, $C(CH_3)_3$), 0.34 (s, 6H, Me_{Si}), −0.08 (s, 6H, Me_{Sn}, $J(^1H-^{119}Sn)$ 51 Hz).

3.6. *rac*-4,4′-Spiro-bis(2,6-di-*tert*-butyl-8,8-dimethyl-8-sila-4-stanna-tetrahydro-*s*-indacene) (**3A**)

A solution of 1.0 ml (6 mmol) of $Sn(NMe_2)_4$ in 50 ml of diethyl ether was added dropwise, over a period of 30 min, to a solution of 3.3 g (11 mmol) of dimethyl-bis(3-*tert*-butyl-cyclopentadienyl)silane in 100 ml Et_2O. After stirring overnight, the reaction mixture was evaporated in vacuo to a volume of 80 ml and stirred again until the NMR signals of $Sn(NMe_2)_4$ were no longer observable. The solvent was then completely evaporated in vacuo and replaced with 30 ml of pentane. The light-yellow precipitate was collected by filtration and washed with small amounts of cold pentane. The mother liquor was reduced in volume and stored again at −30 °C to give further crops of the precipitate, altogether, 2.91 g (4.1 mmol, 74% theoretical yield) of crystalline compound **3A**, which is somewhat air-sensitive, but much less so than the tetrahydro-8-sila-4-stanna-indacenes **2A**–**D**. ^{1}H-NMR ($CDCl_3$, 600 MHz): δ 7.04 (s, 4H, H–C_5, $J(^1H-^{119}Sn)$ 17 Hz), 6.12 (s, 4H, H–C_5, $J(^1H-^{119}Sn)$ 9 Hz), 3.50 (s, 4H, H–C_5, $J(^1H-^{119}Sn)$ 103 Hz), 1.23 (s, 36H, $C(CH_3)_3$), 0.37 (s, 12H, $SiCH_3$). ^{13}C-NMR, broad-band decoupled ($CDCl_3$, 150 MHz): δ 154.2 (C_5, sp^2), 145.2 (C_5, sp^2), 137.4 (C_5, sp^2), 126.6 (C_5, sp^2), 58.9 (C_5, sp^3, $J(^{13}C-^{119}Sn)$ 90 Hz), 32.1 ($C(CH_3)_3$), 31.1 ($C(CH_3)_3$), −2.2 ($SiCH_3$). ^{119}Sn-NMR, broad-band decoupled ($CDCl_3$): δ −45.3. Anal. Calc. for $C_{40}H_{60}Si_2Sn$: C, 67.12; H, 8.45. Found: C, 67.17; H, 8.78%.

3.7. Crystal structure determinations

X-ray diffraction analysis was carried out on a Siemens P4 four-circle diffractometer using Mo–K_α radiation (71.073 pm) and a graphite monochromator (Table 4). Crystal decay was monitored by measuring three standard reflections every 100 reflections. The structures were solved using direct methods [23]. All non-hydrogen atoms were refined anisotropically by least-squares procedures based on F^2 [24], with exception of the disordered carbon atoms in **2D**, which were refined isotropically with bond lengths restrained to be similar. Occupation factors for the disordered *tert*-butyl groups refined to ca. 50%. Hydrogen atoms were refined on calculated positions with fixed isotropic U, using riding model techniques. Absorption corrections were applied using psi-scan data.

4. Supplementary material

Crystallographic data for structural analysis (excluding structure factors) have been deposited with the Cambridge Crystallographic Data Centre as supplementary publication nos. CCDC PEDWIE and 160410. Copies of this information may be obtained, free of charge, from The Director, CCDC, 12 Union Road, Cambridge CB2 1EZ, UK (Fax: +44-1223-336033; e-

Table 4
Crystallographic data [a] for complexes **2D** and **3A**

	Complex **2D**	Complex **3A**
Formula	$C_{24}H_{40}SiSn$	$C_{40}H_{60}Si_2Sn\cdot(OC_4H_{10})_{0.5}$
Crystal color and form	Colorless needle	Colorless prism
Crystal system, space group	Monoclinic, $P2_1/c$	Monoclinic, $C/2c$
a (Å)	17.044(3)	37.542(5)
b (Å)	21.940(7)	11.428(2)
c (Å)	13.391(1)	20.663(2)
β (°)	97.07(2)	105.722(9)
Z; V (Å^3)	8; 4970(2)	8; 8534(2)
Crystal size (mm)	0.2 × 0.3 × 0.3	0.3 × 0.5 × 0.6
T (K); D_{calc} (g cm^{-3})	225; 1.271	243; 1.172
μ (mm^{-1}), $F(000)$	1.082, 1984	0.682, 3192
Scan mode; θ range (°)	$\omega-2\theta$; 2.1–24.0	ω; 2.1–27.0
Reflections collected	7664	9268
Independent reflections	7663	9262
Observed reflections ($I > 2\sigma(I)$)	4349	7486
Number of parameters; goodness-of-fit	466; 1.014	406; 1.084
$R(F)$, $R_w(F^2)$ [a] (observed data)	5.12%, 10.51%	3.29%, 7.70%
$R(F)$, $R_w(F^2)$ [a] (all data)	11.64%, 13.49%	4.77%, 8.47%
Largest difference peak (e Å^3)	0.564	0.401

[a] Weighting scheme: **2D**: $w^{-1} = \sigma^2(F_o^2)+(0.047P)^2+6.38P$, **3A**: $w^{-1} = \sigma^2(F_o^2)+(0.037P)^2+8.81P$, with $P = (F_o^2+2F_c^2)/3$.

mail: deposit@ccdc.cam.ac.uk or www: http://www.ccdc.cam.ac.uk).

Acknowledgements

We thank Dr. Armin Geyer and Ms. Monika Cavegn for help with obtaining and interpreting HMQC and ROESY spectra and Ms. Burckhardt-Boer for elemental analysis. Financial support of this work by BMBF, BASF AG and by funds of the University of Konstanz is gratefully acknowledged.

References

[1] F.R.W.P. Wild, L. Zsolnai, G. Huttner, H.H. Brintzinger, J. Organomet. Chem. 232 (1982) 233.
[2] R.L. Halterman, Chem. Rev. 92 (1992) 965.
[3] H.H. Brintzinger, D. Fischer, R. Mülhaupt, B. Rieger, R. Waymouth, Angew. Chem. 107 (1995) 1255.
[4] L. Resconi, L. Cavallo, A. Fait, F. Piemontesi, Chem. Rev. 100 (2000) 1253.
[5] G.M. Diamond, R.F. Jordan, J.L. Petersen, Organometallics 15 (1996) 4030.
[6] J.N. Christopher, G.M. Diamond, R.F. Jordan, J.L. Petersen, Organometallics 15 (1996) 4038.
[7] G.M. Diamond, R.F. Jordan, J.L. Petersen, Organometallics 15 (1996) 4045.
[8] X. Zhang, Q. Zhu, I.A. Guzei, R.F. Jordan, J. Am. Chem. Soc. 122 (2000) 8093.
[9] H.-R.H. Damrau, E. Royo, S. Obert, F. Schaper, A. Weeber, H.H. Brintzinger, Organometallics 20 (2001) 5258.
[10] I.E. Nifant'ev, P.V. Ivchenko, Organometallics 16 (1997) 713.
[11] I.E. Nifant'ev, P.V. Ivchenko, L. Resconi, European Patent Application 722 950 to Montell, 1996.
[12] L. Resconi, F. Piemontesi, I. Camurati, D. Balboni, Organometallics 15 (1996) 5046.
[13] R. Lisowsky, European Patent Application 669 340 to Witco, 1995.
[14] I.E. Nifant'ev, Organometallics 11 (1992) 3942.
[15] M. Hüttenhofer, M.H. Prosenc, U. Rief, F. Schaper, H.H. Brintzinger, Organometallics 15 (1996) 4816.
[16] I.M. Thomas, Can. J. Chem. 39 (1961) 1386.
[17] K. Jones, M.F. Lappert, J. Chem. Soc. (1965) 1944.
[18] M.A. Lyle, S.R. Stobart, Inorg. Synth. (1977) 178.
[19] M. Hüttenhofer, F. Schaper, H.H. Brintzinger, Angew. Chem. Int. Ed. Engl. 37 (1998) 2268.
[20] H. Wiesenfeldt, A. Reinmuth, E. Barsties, K. Evertz, H.H. Brintzinger, J. Organomet. Chem. 369 (1989) 359.
[21] A. Reinmuth, Dissertation, Universität Konstanz, 1992.
[22] M. Hüttenhofer, Dissertation, Universität Konstanz, 1998.
[23] G.M. Sheldrick, SHELXS-86, University of Göttingen, Germany, 1986.
[24] G.M. Sheldrick, SHELXL-93, University of Göttingen, Germany, 1993.